

# Weakly Supervised Multi-Task Representation Learning for Human Activity Analysis Using Wearables

TAORAN SHENG, The University of Texas at Arlington, USA

MANFRED HUBER, The University of Texas at Arlington, USA

Sensor data streams from wearable devices and smart environments are widely studied in areas like human activity recognition (HAR), person identification, or health monitoring. However, most of the previous works in activity and sensor stream analysis have been focusing on one aspect of the data, e.g. only recognizing the type of the activity or only identifying the person who performed the activity. We instead propose an approach that uses a weakly supervised multi-output siamese network that learns to map the data into multiple representation spaces, where each representation space focuses on one aspect of the data. The representation vectors of the data samples are positioned in the space such that the data with the same semantic meaning in that aspect are closely located to each other. Therefore, as demonstrated with a set of experiments, the trained model can provide metrics for clustering data based on multiple aspects, allowing it to address multiple tasks simultaneously and even to outperform single task supervised methods in many situations. In addition, further experiments are presented that in more detail analyze the effect of the architecture and of using multiple tasks within this framework, that investigate the scalability of the model to include additional tasks, and that demonstrate the ability of the framework to combine data for which only partial relationship information with respect to the target tasks is available.

CCS Concepts: • **Computing methodologies** → **Learning latent representations**; *Multi-task learning*; *Neural networks*; • **Human-centered computing** → *Ubiquitous computing*.

Additional Key Words and Phrases: Weakly supervised learning, Wearable sensors, Activity recognition, Person identification

## ACM Reference Format:

Taoran Sheng and Manfred Huber. 2020. Weakly Supervised Multi-Task Representation Learning for Human Activity Analysis Using Wearables. *Proc. ACM Interact. Mob. Wearable Ubiquitous Technol.* 4, 2, Article 57 (June 2020), 18 pages. <https://doi.org/10.1145/3397330>

## 1 INTRODUCTION

The increased availability of sensors embedded in the environment and worn on the body opens up a vast potential to improve many aspects of life and the workplace, including health management, assistive technology, and workplace safety and efficiency. To realize this potential, it is essential to address the arising need for improved human activity analysis from the sensor data stream. Many different methods have been developed to address this need. While current machine learning methods have achieved impressive results, most of these methods have limitations in the following perspectives: (i) The methods focus on one aspect of the data by either only recognizing the activity [41] or only identifying the person who performed the activity [28]; (ii) Most current person identification methods are based on iris, face, fingerprint or gait identification, in which specific input or activity is needed from the user side [11, 24]; (iii) Pure supervised training of the model is used which requires

---

Authors' addresses: Taoran Sheng, The University of Texas at Arlington, 500 UTA Blvd, Arlington, Texas, USA, 76019-0015, taoran.sheng@mavs.uta.edu; Manfred Huber, The University of Texas at Arlington, 500 UTA Blvd, Arlington, Texas, USA, 76019-0015, huber@cse.uta.edu.

---

Permission to make digital or hard copies of all or part of this work for personal or classroom use is granted without fee provided that copies are not made or distributed for profit or commercial advantage and that copies bear this notice and the full citation on the first page. Copyrights for components of this work owned by others than ACM must be honored. Abstracting with credit is permitted. To copy otherwise, or republish, to post on servers or to redistribute to lists, requires prior specific permission and/or a fee. Request permissions from [permissions@acm.org](mailto:permissions@acm.org).

© 2020 Association for Computing Machinery.

2474-9567/2020/6-ART57 \$15.00

<https://doi.org/10.1145/3397330>

large amounts of labeled data [25], that is often hard to come by, especially in personalized applications; (iv) Most previous methods rely heavily on data that is labeled with respect to all aspects of the task and thus make it difficult to combine datasets that were created for different purposes, even if they were collected in the same environment, since each dataset would only contain the labels for that specific task. As a result, significant amounts of costly re-labeling would be required which might not even be possible in many real world scenarios since the required information for the labeling is no longer available in the data.

This paper presents an approach that attempts to mitigate these limitations. Intuitively, different persons perform activities in different ways. Distinct personal characteristics are commonly present in all the activities performed by the person. Thus, identifying a person with different types of activities can generalize the model to activity-based identification which does not need a specific user's cooperation. Moreover, from the multi-task perspective, sharing knowledge between related tasks leads to learning generalized representations, helping to reduce the risk of overfitting one specific task. Since human activity recognition (HAR) and person identification are closely related, combining them into one multi-task model is reasonable and can be beneficial for both tasks. Furthermore, while learning of a selective representation is commonly achieved by supervised training, previous works in computer vision [9, 19] have shown the possibility to achieve similar performance in a weakly supervised manner while dramatically reducing the effort needed to obtain training data.

Based on these observations, this paper proposes a unified deep learning architecture centered around siamese networks and temporal convolutions for simultaneous HAR and activity-based person identification, which is trained using only the information about the similarity of the activities and the persons without knowing the explicit labels. Moreover, the developed architecture is non task-specific, easily extendable to larger numbers of tasks, and can be trained with data where only partial similarity information is available, i.e. where each data item only contains relationship information for a subset of the tasks that the system is to be trained for.

To demonstrate the potential and scalability of the proposed model and to evaluate its effectiveness in different scenarios, a number of experiments are presented and analyzed: (i) To evaluate the proposed method, the framework is applied to the HAR and person identification problem and compared to existing single and multi-task approaches in these domains. The results and visualization of the formed representation space confirm that our method can learn them successfully, and comparison with state-of-the-art methods, including fully supervised methods that take advantage of additional, explicit labels, demonstrate that our method can achieve competitive performance on several datasets; (ii) To assess the scalability of the proposed method, we expand the model to learn representations for additional attributes in the data along with HAR and person identification. These experiments show that the proposed architecture can scale to increasing numbers of tasks with very little loss of accuracy; (iii) Ablation studies are provided to investigate the influence of multi-task learning within the architecture, demonstrating not only that multiple tasks can be learned but that training for multiple tasks often increases the performance for individual tasks; (iv) To investigate the impact of data that has only partial similarity information, an experiment is performed where each data item only contains similarity information with respect to one of the tasks and only to a subset of the data. The results here show that the proposed model can successfully learn all tasks even with partial similarity information with a performance that is close to the one with full information.

## 2 RELATED WORK

### 2.1 HAR and Person Identification

There are two main directions in wearable sensor-based HAR, either handcrafted feature-based methods or deep neural network (DNN) based methods. Handcrafted features are designed with domain knowledge. For example, [3, 31] used statistical features, such as mean, variance and entropy, in their models. Features extracted from a wavelet transform were utilized in [34]. He and Jin [15] used features extracted by applying discrete

cosine transform. The advantage of these features is that they can be derived from the signal easily and have been shown to be effective in the HAR system. However, domain knowledge is required to design the features manually. Recently, many HAR models adopt DNN to allow automatic feature extraction. Morales and Roggen [25] proposed a model consisting of convolutional neural network (CNN) and long short-term memory (LSTM) components. CNN is used here to capture local temporal relations while the memory states of LSTM ease the learning of long time scale dependencies. In [1], a hybrid approach was proposed, which used a deep belief network as an emission matrix of a Hidden Markov Model to model the sequence of human activities. These methods can automatically extract features from the data without any domain knowledge. But, they still require explicit labels to supervise the training of the model.

Many person identification methods are based on iris, face, and fingerprint. Those kinds of methods require specific cooperation or explicit action/input from the user side, e.g. standing in front of a camera, looking at a specific point, etc. [10], while gait recognition-based person identification, e.g. [11, 17, 23], enables an inexpensive, convenient, and unobtrusive way to complete the task. However, gait-based methods assume that walking is the only activity to be performed during the identification. In many real-world applications, this assumption may not hold. There have been only a few studies that are identifying the person based on various activities recorded by sensors. Kwapisz, Weiss, and Moore [28] proposed a model which used handcrafted features and decision trees. Their model addressed the biometric identification task by analyzing four types of dynamic activities (walking, jogging, ascending and descending stairs). Elkader et al [10] expanded the person identification method from a limited number of specific activities to a set of various normal daily activities. However, these works still focus on only one aspect of the data.

The most closely related works are perhaps [16, 29]. In [29], Reddy et al. proposed a method to first identify the person's states: standing, sitting, or walking, then separate SVM based models are used for identifying the person for each of the three mentioned states. This method addresses posture recognition and person identification, but the two tasks are addressed in two separate steps by separate models. Hernandez, McDuff, and Picard [16] collected experimental data from a wrist worn smartwatch, and their proposed model identifies the person and three static body postures (sitting, standing, and lying) at the same time. These two works address two tasks, but while the first uses walking for activity recognition, in both cases the methods for person identification are based solely on a very small number of simple static postures, and no information about the dynamics of activities is used for this task. Hence, these two methods do not support general activity-based person identification. Moreover, both use a very small set of activities and are not easily expandable to a more general set, and do not provide any explicit means to add additional attributes or tasks. In contrast, the framework presented here does not make any assumptions about the type of activities and provides a uniform, consistent model for multi-task learning of both static and dynamic attributes. For this, it develops a novel siamese network training architecture that allows efficient training of a latent representation that accurately embeds the chosen attributes. In addition, it extends the state-of-the-art by permitting the system to be trained without explicit labels, just using similarity or relationship information, as well as to be trained with datasets that only contain partial similarity information.

## 2.2 Siamese Networks and Temporal Convolution Networks

We take inspiration from siamese architectures and temporal convolutional networks (TCN) to design our model that can efficiently capture the temporal patterns and compute the semantic similarity between the pairs of data sequences.

A siamese network [8] is a neural network with dual branches and shared weights. As illustrated in Fig. 1, it processes an input pair  $\{x_a, x_b\}$  and yields a pair of comparable representation vectors  $\{H_a, H_b\}$ . The distance between the comparable representation vectors is then used as the semantic similarity of the input pair. The siamese architecture is widely used in many domains. Originally [8], a siamese network was used to verify

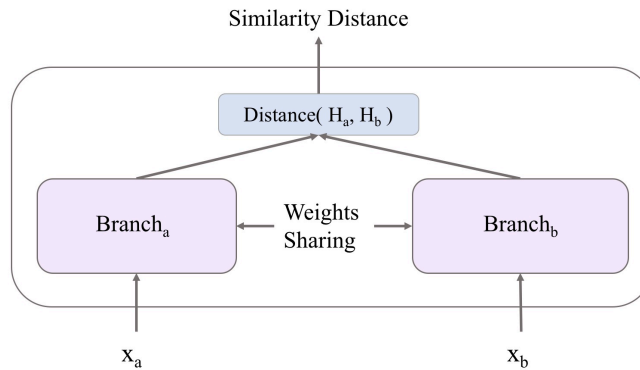


Fig. 1. The basic architecture of a siamese network.

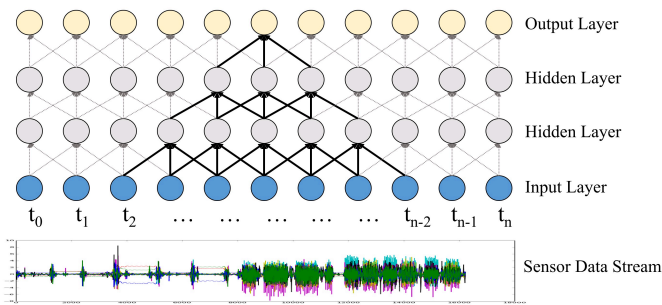


Fig. 2. The basic architecture of a temporal convolutional network (TCN).

signatures. Mueller and Thyagarajan [26] used a siamese recurrent neural network to measure the semantic similarity between a pair of sentences. In [9], a siamese CNN is proposed to learn a complex similarity metric for face verification. In other areas, the siamese architecture has been applied in unsupervised acoustic model learning [18, 33, 39], image recognition [7] and object tracking [19].

A TCN uses a hierarchy of convolutions to abstract the temporal relations of the data stream at different time scales. As shown in Fig. 2, the hierarchical structure of the TCN is effective to learn the incrementally longer-range temporal patterns in the data stream with each increase in the depth of the network. More specifically, the low-level TCN layers focus on capturing simple features within a short period of time, while the high-level layers learn to aggregate the low-level simple features into more complex and abstract high-level concepts within a longer period of time. Hence, stacking TCN layers together is an efficient way to model the longer-range temporal patterns in the data. TCN has been successfully applied in many different areas, e.g., computer vision (video data stream), natural language processing (speech or text data), etc. In [35], Oord et al. proposed a model that can generate raw speech signals. In [21, 22], TCN has been used to segment and detect action in the video. In [42], a character-level TCN is used to classify text.

### 3 PROPOSED METHOD

Our work differs from previous works in several important ways. First, unlike most of the previous methods, our proposed model can identify the activity and the person simultaneously and can be systematically expanded

to identify additional types of attributes. Second, in comparison to most of the previous wearable sensor-based person identification methods, which have been customized to either only focused on gait information, or only used a limited number of dynamic activities or static body postures, our model uses a task-agnostic structure and is here evaluated on four diverse public datasets [5, 20, 30, 31]. These datasets, respectively, contain 12, 12, 7, or 6 types of different activities performed by 9, 10, 30, or 36 different persons. This evaluation offers a more realistic and challenging scenario, and through the use of a wider range of activities may lead to a more robust identification model. Moreover, since in the daily routine of a person in real life many different activities will be performed, an identification system that is restricted to a very small number of activities might fail to work, and even in situations where it can still make correct classifications can only take advantage of a small part of the available data. Third, our proposed method is capable of learning with data with only partial similarity or data relationship information, which could be useful in many real-world applications where not all attributes of the data can be determined for any given point in time or where multiple datasets that were collected for different purposes using the same sensors in the same domain can be combined to obtain a larger training set and consequently better task performance and less risk of overfitting. Finally, our method, by taking advantage of the siamese architecture, can be trained in a weakly supervised manner, hence no explicit labels are needed.

To achieve these capabilities, we frame the problem as learning an invariant mapping that maps the input data sequence into a semantic representation space. The learning process relies only on the relationship of the data sequences in the input pair, therefore the learned model will map two data sequences either to the same area in the representation space if the two data sequences are semantically similar, or to different areas if the data sequences are semantically dissimilar. Formally, given a pair of sensor data sequences  $\{x_a, x_b\}$ , the aim is to learn a mapping  $f$  that maps the pair  $\{x_a, x_b\}$  into a representation space such that:

$$H_{x_a} = f(x_a) \quad (1)$$

$$H_{x_b} = f(x_b) \quad (2)$$

The distance between the representation pair  $\{H_{x_a}, H_{x_b}\}$  approximates the semantic similarity of the input pair  $\{x_a, x_b\}$ . Specifically, our proposed model learns two such mappings:

$$f^{act} : \begin{cases} x_a \rightarrow H_{x_a}^{act} \\ x_b \rightarrow H_{x_b}^{act} \end{cases} \quad (3)$$

$$f^{pers} : \begin{cases} x_a \rightarrow H_{x_a}^{pers} \\ x_b \rightarrow H_{x_b}^{pers} \end{cases} \quad (4)$$

The mapping  $f^{act}$  is based on the activity similarity of  $x_a$  and  $x_b$ , such that if  $x_a$  and  $x_b$  belong to the same type of activity, then  $H_{x_a}^{act}$  and  $H_{x_b}^{act}$  will stay together, while  $H_{x_a}^{act}$  and  $H_{x_b}^{act}$  will stay away from each other, if  $x_a$  and  $x_b$  are from different types of activities. The mapping  $f^{pers}$  is based on the performer of the activity, such that if  $x_a$  and  $x_b$  are performed by the same person, then  $H_{x_a}^{pers}$  and  $H_{x_b}^{pers}$  will stay together, while  $H_{x_a}^{pers}$  and  $H_{x_b}^{pers}$  will stay away from each other if  $x_a$  and  $x_b$  are performed by different persons. The mappings  $f^{act}$  and  $f^{pers}$  preserve different semantic relationships between the input data sequences. The proposed model learns these two mappings at the same time.

### 3.1 TCN Blocks

Suppose, we are given a pair of sensor data sequences  $\{x_a, x_b\}$ :  $x_a = (x_{a_1}, \dots, x_{a_{\tau'}})$  and  $x_b = (x_{b_1}, \dots, x_{b_{\tau''}})$ , where  $\tau'$  and  $\tau''$  denote the time length of the signals and  $x_{a_t} = [s_t^1, \dots, s_t^n]$  is the  $n$ -dimensional sensor reading in sequence

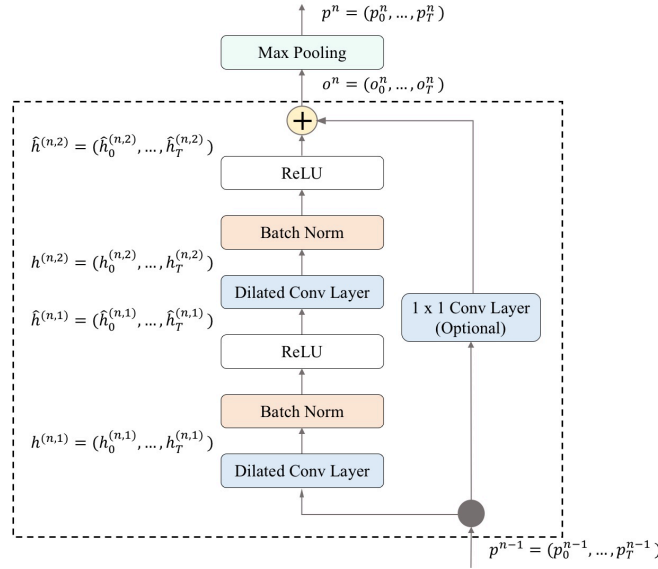


Fig. 3. A TCN block with two convolutional layers.

$x_a$  at time  $t$ . The learned mappings are then defined as follows:

$$f^{act} : \begin{cases} (x_{a_1}, \dots, x_{a_{t'}}) \rightarrow H_{x_a}^{act} \\ (x_{b_1}, \dots, x_{b_{t'}}) \rightarrow H_{x_b}^{act} \end{cases} \quad (5)$$

$$f^{pers} : \begin{cases} (x_{a_1}, \dots, x_{a_{t'}}) \rightarrow H_{x_a}^{pers} \\ (x_{b_1}, \dots, x_{b_{t'}}) \rightarrow H_{x_b}^{pers} \end{cases} \quad (6)$$

The TCN architecture is adopted as the basic building block for abstracting the sequence due to its ability to efficiently abstract time series data at different time scales. As illustrated in Fig. 3, each TCN block is composed of a series of transformations, which includes the dilated temporal convolutions with dilation rate  $d$ , batch normalization, non-linearity  $g(\cdot)$ , and residual connection  $\oplus$ . Assume that the proposed model contains a sequence of  $N$  TCN blocks where each block contains  $L$  convolutional layers with  $m$  different feature maps of width  $k$ , and the parameters of the feature maps are  $w$ . For the  $n^{\text{th}}$  block, the input  $p^{n-1}$  is the max-pooled output from the  $(n-1)^{\text{th}}$  block, and the temporal convolutions that we apply in each TCN block to capture the patterns over the course of an activity are constructed from the following components.

**3.1.1 Dilated Convolutional Layer.** The advantage of dilated convolutions is that they support faster expanding receptive fields without losing resolution or coverage [38]. Batch Normalization (BN) is applied after each dilated convolutional layer and before the non-linear activation function. BN can accelerate the learning process by reparameterizing the underlying optimization problem to make it more stable and smooth [32]. Formally, in the  $l^{\text{th}}$  convolutional layer of the TCN block, the computation is then defined as follows:

$$h_t^{(n,l)} = \begin{cases} \sum_{i=-\frac{k-1}{2}}^{\frac{k-1}{2}} w_i \cdot p_{t-d \cdot i}^{n-1} & \text{if } l = 1. \\ \sum_{i=-\frac{k-1}{2}}^{\frac{k-1}{2}} w_i \cdot \hat{h}_{t-d \cdot i}^{(n,l-1)}, & \text{otherwise.} \end{cases} \quad (7)$$



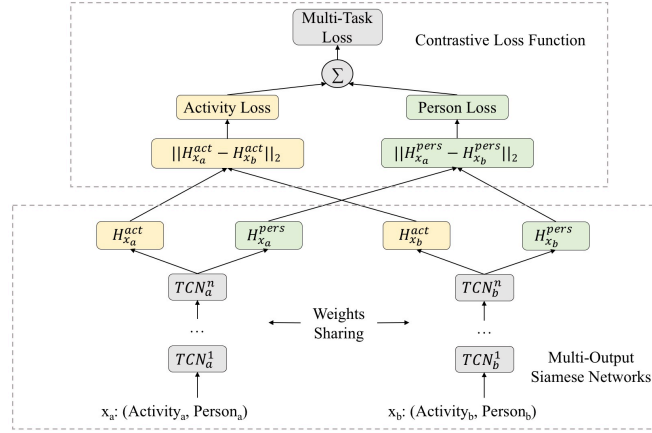


Fig. 4. A dual-output siamese network.

$$\hat{h}_t^{(n,l)} = g(h_t^{(n,l)}) \quad (8)$$

where  $h^{(n,l)}$  is the output of the convolutions and  $\hat{h}^{(n,l)}$  is the output of the non-linear activation function.

**3.1.2 Residual Connections.** The output of the TCN block,  $o^n$ , is the sum of the result of the last convolution  $\hat{h}_t^{(n,L)}$  and the input of the block,  $p^{n-1}$ . However, in TCN blocks, the shapes of the input tensor and the output tensor can be different [4]. To address this problem, if  $\hat{h}_t^{(n,L)}$  and  $p_t^{n-1}$  have different shapes, a  $1 \times 1$  convolution will be used as the residual connection. Otherwise, an identity function will be used as the residual connection:

$$o_t^n = \hat{h}_t^{(n,L)} \oplus p_t^{n-1} \quad (9)$$

The temporal max pooling with width 2 is used between two consecutive TCN blocks to reduce the size of the time dimensions while introducing slight translational invariance in time:

$$p_t^n = \max(o_{t-1}^n, o_t^n) \quad (10)$$

### 3.2 Multi-Output Siamese Networks

The architecture of the proposed model is outlined in Fig. 4. It contains two networks  $TCN_a$  and  $TCN_b$ . Each network has  $n$  TCN blocks, shares the weights, and processes one of the data sequences in the input pair  $\{x_a, x_b\}$ . In order to disentangle the activity and person information extracted by the TCN networks, two fully-connected (FC) layers are connected to the TCN networks and are responsible to process the activity representations  $\{H_{x_a}^{act}, H_{x_b}^{act}\}$  and person representations  $\{H_{x_a}^{pers}, H_{x_b}^{pers}\}$ , respectively. The weights of the FC layers are shared within the same representation learning task.

This model is trained using 4-tuples  $\{x_a, x_b, y^{act}, y^{pers}\}$ , where  $x_a$  and  $x_b$  are the data sequences of the input pair.  $y^{act}, y^{pers} \in \{0, 1\}$  denote the semantic relationships of the input pair, where  $y^{act} = 0$  or  $y^{pers} = 0$  denotes that  $\{x_a, x_b\}$  is a semantically negative pair, i.e. they are maximally dissimilar in terms of the corresponding property. If  $y^{act} = 0$ ,  $x_a$  and  $x_b$  are different kinds of activities; if  $y^{pers} = 0$ ,  $x_a$  and  $x_b$  are performed by different persons.  $y^{act} = 1$  or  $y^{pers} = 1$  denotes that  $\{x_a, x_b\}$  is a semantically positive pair. If  $x_a$  and  $x_b$  are the same kind of activity,  $y^{act} = 1$ ; if  $x_a$  and  $x_b$  are performed by the same person,  $y^{pers} = 1$ .

### 3.3 Contrastive Loss Function

Given the input pair  $\{x_a, x_b\}$ , the model outputs a pair of activity representations,  $\{H_{x_a}^{act}, H_{x_b}^{act}\}$ , and a pair of person representations  $\{H_{x_a}^{pers}, H_{x_b}^{pers}\}$ . The loss function used to train the model is also defined on the pairs. The similarity distance  $Dist_s$  between the input pair is measured by the euclidean distance between their representation pair:

$$Dist_s(x_a, x_b) = \|H_{x_a} - H_{x_b}\|_2 \quad (11)$$

To make the notation clearer,  $Dist_s(x_a, x_b)$  is rewritten as  $D$ . Then the loss function for each of the categorizations used for training is defined as:

$$L(x_a, x_b, y) = \sum_{i=1}^N L^i(x_a^i, x_b^i, y^i) \quad (12)$$

$$L^i(x_a^i, x_b^i, y^i) = y^i L_s(x_a^i, x_b^i) + (1 - y^i) L_d(x_a^i, x_b^i) \quad (13)$$

where  $(x_a^i, x_b^i, y^i)$  is the  $i$ -th sample in the data set.  $L_s, L_d$  are the loss terms for the positive pair ( $y = 1$ ) and the negative pair ( $y = 0$ ). The forms of  $L_s, L_d$  are given by:

$$L_s = \frac{1}{2}(D)^2 \quad (14)$$

$$L_d = \frac{1}{2}\{\max(0, \delta - D)\}^2 \quad (15)$$

where  $\delta$  is a margin hyperparameter. It defines that the negative pairs contribute to the loss function if their distance is smaller than the margin  $\delta$ . Then, the loss function is applied in each representation space, and the weighted sum of the loss function in each representation space is defined for the final multi-task model ( $\alpha$  and  $\beta$  are the corresponding weights for each task):

$$\begin{aligned} \mathcal{L}(x_a, x_b, y^{act}, y^{pers}) = \\ \alpha \cdot L^{act}(x_a, x_b, y^{act}) + \beta \cdot L^{pers}(x_a, x_b, y^{pers}) \end{aligned} \quad (16)$$

To train the network, we use the standard backpropagation algorithm with stochastic gradient descent. All the parameters are initialized to small values. The start learning rate is  $lr = 0.05$  and an exponential decay function is applied to the learning rate every 10000 steps with a decay rate of 0.95. The network is tested on validation data after each epoch. If the validation error stopped decreasing for a predefined number of epochs, training is finished.

### 3.4 Cluster Construction

After all the parameters are learned, we can use the trained model to provide metrics for a wide range of different clustering algorithms. Because the trained model can map the data sample  $x$  into the representation space, where the representation vector  $H$  is positioned such that data with the same semantic meaning are located close to each other, clusters in this space should capture the corresponding property. More specifically, in our experiments, the trained model maps the data samples into the activity representation space and the person representation space. In the activity representation space, the data samples will be grouped into clusters according to the activity type. In the person representation space, the data samples will be grouped into clusters according to the identity of the person. Hence, after mapping the data samples to the more clustering-friendly representations, different clustering algorithms can be used on these learned representations. In our experiments, K-means is employed as the clustering method.



## 4 EVALUATION AND EXPERIMENTS

In order to evaluate the effectiveness of the proposed model, we use four public datasets that contain raw sensor data sequences of different human activities performed by different persons. We conduct activity clustering and person clustering on the learned representations as described in Section 3.4.

### 4.1 Datasets

The datasets used here are selected from widely used benchmark datasets [37] as the ones that contain a good number of different persons performing numerous diverse activities. Those datasets are recorded by various sensors, e.g. accelerometer, gyroscope, magnetometer etc, and include human activities in different scenarios. All the sensor data sequences are segmented with a sliding window as described with each of the datasets below.

The **PAMAP2** dataset is collected from 9 participants performing 12 activities over a total of 10 hours. It includes sport exercises (rope jumping, nordic walking etc), and household activities (vacuum cleaning, ironing etc). One heart-rate monitor and three inertial measurement units (IMUs) located on the chest, dominant wrist and ankle were used to record the heart rate, accelerometer, gyroscope, magnetometer, and temperature data. We replicate previous work [14, 40] to downsample the data from 100Hz to 33.3Hz, and use a sliding window of 5.12 seconds with one second step size.

The **MHEALTH** dataset contains data recorded from 10 volunteers carrying out 12 physical activities, including primitive body parts movements (waist bends forward, frontal elevation of arms etc), and composite body movements (cycling, jumping front and back etc). The data is collected by using three sensors placed on the subject's chest, right wrist and left ankle to record accelerometer, gyroscope, and magnetometer signals. The chest sensor also records 2-lead ECG signals. The sampling rate of all sensing modalities is 50Hz. As in previous work [27], we use a sliding window of 5 seconds with a step size of 2.5 seconds.

The **SBHAR** dataset provides data gathered from 30 participants performing 6 basic activities, such as walking and lying, and 6 postural transitions, such as stand-to-sit, sit-to-lie. In our experiment, we consider all the postural transitions as one general transition. The data was collected by placing a smartphone on the waist of the participant, and the inertial sensors in the smartphone were used to record the accelerometer and gyroscope data at a sampling rate of 50Hz. As used in the previous work [31], we use a sliding window of 2.56 seconds with a step size of 1.28 seconds.

The **WISDM** dataset contains data collected with one accelerometer in a smartphone from 36 volunteers carrying out 6 activities, including jogging, climbing stairs, etc. The sampling rate is 20Hz. We use the same settings as used in [20] to set the sliding window size to be 10 seconds without overlap.

### 4.2 Performance Metrics

To compare with previous works, we use mean F1-score ( $F_m$ ) and clustering accuracy as the metrics.  $F_m$  is defined as follows:

$$F_m = \frac{2}{|C|} \sum_{i=1}^C \frac{Precision_i \cdot Recall_i}{Precision_i + Recall_i} \quad (17)$$

where  $i = 1, \dots, C$  is the set of classes. For the given class  $i$ ,  $Precision_i = \frac{TP_i}{TP_i + FP_i}$ ,  $Recall_i = \frac{TP_i}{TP_i + FN_i}$ ;  $TP_i$  and  $FP_i$  denote the number of true positives and false positives, and  $FN_i$  is the number of false negatives.

### 4.3 Results

We used the same model architecture with 3 TCN blocks across all the experiments. A shorthand description of the shared layers is: TCN (128) – P– TCN (128) – P– TCN (128), where TCN(128) denotes a TCN block with 128 feature maps, and  $P$  a max-pooling layer. The internal structure of a TCN block is the same as illustrated

Table 1. Results on PAMAP2 in terms of  $F_m$ 

Methods	Activity	Person
Probability SVM [31]	0.9304	-
Probability SVM with Filter [31]	0.9433	-
LSTM-F [14]	0.9290	-
CNN [14]	0.9370	-
DNN [14]	0.9040	-
State + Person SVMs [29]	0.9384	0.9123
PCA + k-Means	0.4244	0.2040
3-NN	-	0.9416
5-NN	-	0.9014
Decision Tree	-	0.9781
Proposed Multi-Task Method	<b>0.9893</b>	<b>0.9881</b>

Table 2. Results on MHEALTH in terms of Accuracy

Methods	Activity	Person
CNN-1D [13]	0.9809	-
CNN-2D [13]	0.9829	-
CNN-pff [12]	0.9194	-
FE-AT [27]	0.9664	-
State + Person SVMs [29]	0.8376	0.6777
PCA + k-Means	0.4850	0.2361
3-NN	-	0.8540
5-NN	-	0.8380
Decision Tree	-	0.6714
Proposed Multi-Task Method	<b>0.9957</b>	<b>0.9948</b>

Table 3. Results on SBHAR in terms of Accuracy

Methods	Activity	Person
Probability SVM [31]	0.9580	-
Probability SVM with Filter [31]	0.9678	-
CNN [6]	0.9870	-
State + Person SVMs [29]	0.9034	0.5614
PCA + k-Means	0.5282	0.1299
3-NN	-	0.5330
5-NN	-	0.5123
Decision Tree	-	0.4957
Proposed Multi-Task Method	<b>0.9885</b>	<b>0.8892</b>

in Figure 3. In addition, above the last TCN block, one FC layer with 256 hidden nodes is used for each single representation learning task. The experimental results are summarized in Tables 1, 2, 3, and 4.

In addition to previous published works which use fully supervised learning, we also used principal components analysis (PCA), k-nearest neighbors ( $k = 3, 5$ ), and a decision tree algorithm (C4.5) as baselines. As shown in the result tables, our proposed multi-task method achieved competitive performance on both tasks compared with the supervised single-task approaches in most situations. Since most previous methods were applied only to one of the tasks, only the performance results for that task are listed in the tables.

Table 4. Results on WISDM in terms of Accuracy

Methods	Activity	Person
CNN with partial weight sharing [41]	0.9688	-
DBN+HMM [1]	<b>0.9823</b>	-
Decision Tree [20]	0.8510	-
Multilayer Perceptron [20]	0.9170	-
CNN+stat. features [2]	0.9332	-
State + Person SVMs [29]	0.8128	0.5070
PCA + k-Means	0.5181	0.2430
Neural Net* [28]	-	0.6950
Decision Tree* [28]	-	0.7220
3-NN	-	0.2651
5-NN	-	0.2470
Decision Tree	-	0.2189
Proposed Multi-Task Method	0.9576	<b>0.8112</b>

\* Experiment results based on 4 activities.

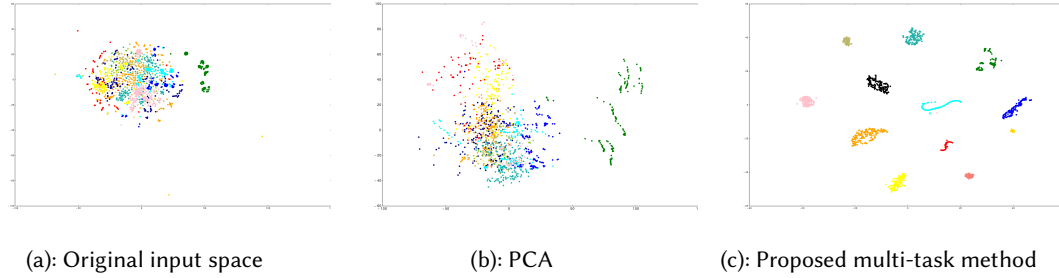


Fig. 5. Visualizations on the activity aspect of PAMAP2.

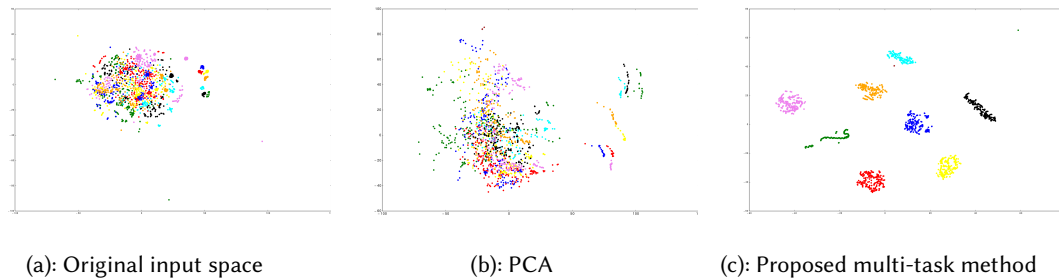


Fig. 6. Visualizations on the person aspect of PAMAP2.

#### 4.4 Visualization and Analysis

To further analyze the representations learned by the proposed multi-task method and compare it with other embedding techniques, we used t-sne [36] to visualize the activity and person representation spaces. Due to the space limitation, we only list the visualizations of the proposed multi-task method and PCA on two representative datasets: PAMAP2 and SBHAR. PAMAP2 contains complex activities, which makes it difficult to model. SBHAR

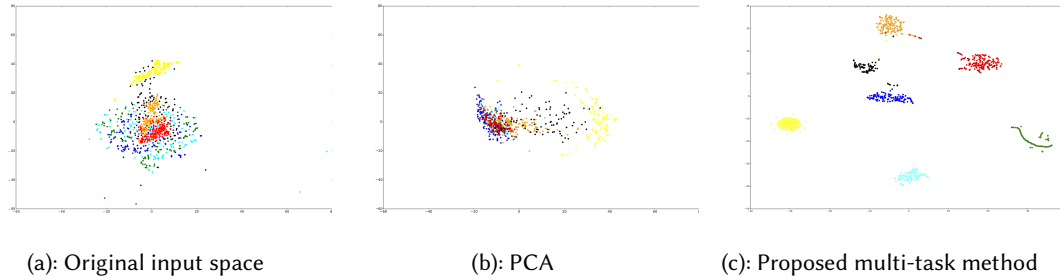


Fig. 7. Visualizations on the activity aspect of SBHAR.

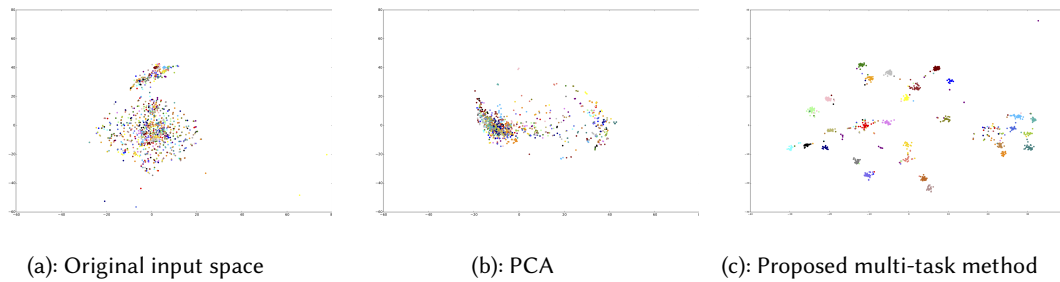
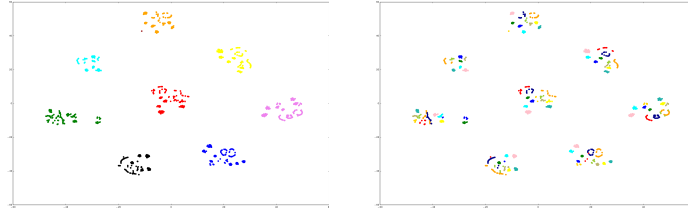


Fig. 8. Visualizations on the person aspect of SBHAR.

contains unbalanced class numbers in the two aspects of the data. In particular, it includes 30 persons who perform 7 activities, which leads to unbalanced sample sets across the two tasks in that there are significantly fewer data samples for the person classes than for the activity classes. This, in turn, leads to bias and difficulties learning these two highly unbalanced tasks simultaneously.

In Fig. 5, 6, 7 and 8, different colors denote different true semantic labels in the datasets. From these figures, we can reach the following conclusions: (i) The proposed multi-task method can effectively disentangle different semantic representations from the data. (ii) The learned representation clusters are compact and clearly separated in each representation space. Thus, downstream tasks like clustering can benefit from it and achieve promising performance. (iii) For those datasets that contain unbalanced class numbers in different aspects of the data, the qualities of the learned representations are also unbalanced. For example, in Fig. 7 and 8, the activity representations are more compact within the same cluster, and different clusters are clearly separated with each other. But in the person representation space, some data samples stay away from their corresponding clusters, and some clusters stay relatively close to each other. The imbalance is also reflected on the performances. As shown in Table 3, the accuracy on the activity recognition task is 10% higher than on the person identification task.

After evaluating the effectiveness of the learned representations for each task, we also visualize the output from TCN, which we consider a more general representation because it is learned by the shared layers in the model without aiming at any specific task. As shown in Fig. 9(a), 9(b), the general representations form a two-level structure. At the higher level, illustrated in Fig. 9(a), the clusters are grouped in accordance with the identity of the persons. At the lower level, shown in Fig. 9(b), in each person's cluster, different activities are further grouped into different smaller sub-clusters.



(a): General rep. colored by persons (b): General rep. colored by activities

Fig. 9. Visualizations on the general representations of PAMAP2.

#### 4.5 Ablation Studies

As the experimental results in Section 4.3 show, the proposed multi-task model can learn the two related tasks (activity recognition and person identification) successfully. To further understand the effect of the multi-task training framework, a series of ablation experiments are performed to separately measure the influence of multi-task learning. In the ablation experiments, the original objective of the multi-task learning is transformed into two separate objectives and two separate single-task learning models are built based on the same underlying siamese network architecture. Thus, each single-task model is trained to learn only one task, namely activity recognition (AR) or person identification (PI). Comparing these to the model trained using multi-task data should provide insight into the benefit of multi-task training and thus any cross-fertilization occurring between the two tasks. The experiment results of the ablation studies are provided in Table 5.

Table 5. Ablation studies on effect of multi-task learning.

Methods	Activity	Person
<b>PAMAP2</b>		
Single-Task Model AR	0.9856	–
Single-Task Model PI	–	0.9812
Proposed Multi-Task Method	<b>0.9893</b>	<b>0.9881</b>
<b>MHEALTH</b>		
Single-Task Model AR	0.9756	–
Single-Task Model PI	–	0.9889
Proposed Multi-Task Method	<b>0.9957</b>	<b>0.9948</b>
<b>SBHAR</b>		
Single-Task Model AR	0.9436	–
Single-Task Model PI	–	0.8138
Proposed Multi-Task Method	<b>0.9885</b>	<b>0.8892</b>
<b>WISDM</b>		
Single-Task Model AR	<b>0.9629</b>	–
Single-Task Model PI	–	0.8080
Proposed Multi-Task Method	0.9576	<b>0.8112</b>

As shown in Table 5, expanding the model from single-task learning to multi-task learning does not cause performance loss and degradation in most cases. On the contrary, the performance of multi-task training is most of the time better than the one of the single-task models. The only exception here is in the case of the WISDM

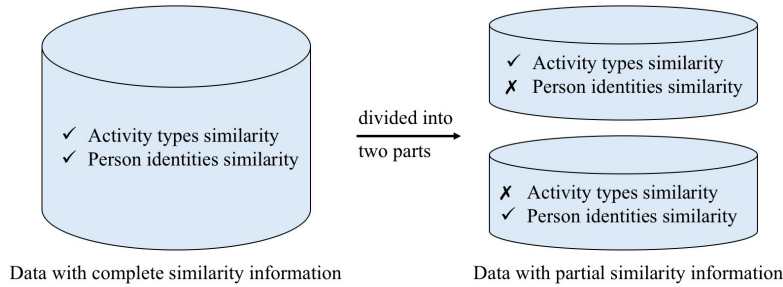


Fig. 10. Generation of data with partial similarity information from the original data for partial information experiments.

dataset where a small drop in accuracy for activity recognition goes along with an increase in accuracy for person identification. One possible reason is that the WISDM dataset is collected with one single accelerometer with a relatively low sampling rate, providing significantly less data per time unit compared to the other datasets. Due to this, the time window used in this dataset is also significantly longer (10 s), leading to a much coarser grained set of labeled data points, making it potentially harder to arrange them in spaces that clearly separate them based on multiple semantic criteria due to the larger amount of overlap in the data. As a result, it might be the case here that the data does not contain sufficient information for learning the more complex multi-task model, necessitating the observed trade-off between activity recognition and person identification. However, it is important to note here that the drop in activity recognition performance is relatively limited and smaller than the obtained gain in person identification accuracy. This result confirms the assumption that activity recognition and person identification are closely related tasks, thus, sharing knowledge and learning a generalized representation between them can be beneficial for both tasks.

#### 4.6 Multi-Task Learning with Partial Similarity Information

Having analyzed the effect of the multi-task framework, we now consider another, more challenging scenario. Previous experiments are all based on the assumption that the similarity information of the activity types and the person identities is fully visible to the model. However, in many real world applications it will be impossible for the model to have complete and perfect information about the similarities between all data items and for all attributes of interest. Therefore, in this section, another additional constraint is imposed on the proposed multi-task method. We conducted experiments where the model is trained with only partial observations of the similarity information about the data. To be more specific, as illustrated in Fig. 10, we divided the dataset into two parts of equal size. One part of the data only provides the similarity information of the activity types, while the other part of the data only provides the similarity information of the person identities. It is important to note here that this implies that no single data item in the training set contained similarity information for both tasks and this can thus be seen as similar to a case where data was separately collected for the two tasks and no re-assessment of the similarity for the other task was performed after collection. Then, the proposed multi-task method is trained to learn both AR and PI tasks with this data. The experimental results are summarized in Table 6.

As shown in Table 6, for both tasks, despite the data only containing partial similarity information for the multi-task model and thus only providing information regarding one task from each sample, the performance of the multi-task method is relatively close to the performance of the multi-task method using the complete similarity information for each data item and outperforms a few single-task learners trained on the data with full information from the ablation study. This indicates that our proposed method, which is trained to learn

Table 6. Multi-task learning with partial similarity information.

Methods	Activity	Person
<b>PAMAP2</b>		
Single-Task Model AR	0.9856	–
Single-Task Model PI	–	0.9812
Proposed Multi-Task Method with Complete Similarity Information	<b>0.9893</b>	<b>0.9881</b>
Proposed Multi-Task Method with Partial Similarity Information	0.9849	0.9879
<b>MHEALTH</b>		
Single-Task Model AR	0.9756	–
Single-Task Model PI	–	0.9889
Proposed Multi-Task Method with Complete Similarity Information	<b>0.9957</b>	<b>0.9948</b>
Proposed Multi-Task Method with Partial Similarity Information	0.9744	0.9643
<b>SBHAR</b>		
Single-Task Model AR	0.9436	–
Single-Task Model PI	–	0.8138
Proposed Multi-Task Method with Complete Similarity Information	<b>0.9885</b>	<b>0.8892</b>
Proposed Multi-Task Method with Partial Similarity Information	0.9618	0.8247
<b>WISDM</b>		
Single-Task Model AR	<b>0.9629</b>	–
Single-Task Model PI	–	0.8080
Proposed Multi-Task Method with Complete Similarity Information	0.9576	<b>0.8112</b>
Proposed Multi-Task Method with Partial Similarity Information	0.9509	0.7791

both tasks with partial similarity information is capable of effectively utilizing cross-task information to achieve performance that is competitive with other models trained with complete similarity information for all tasks.

It is worth to mention that one of the reasons for the model performance loss on SBHAR and WISDM is that these two datasets contain unbalanced class numbers, SBHAR contains 30 persons performing 7 activities and WISDM contains 36 persons performing 6 activities. This leads to the situation where each person class has significantly fewer data samples than an activity class. Moreover, when the datasets are divided into two parts of equal size, each part only contains partial information of the data, and this further reduces the size of the data samples that can be used for the PI task learning. Therefore, without enough training data, the performance of the model will be degraded.

#### 4.7 Attribute Representation Learning

In order to evaluate the scalability and robustness of the method, we also expanded the proposed multi-task model to include additional attribute representation learning. We selected PAMAP2 to evaluate the expanded model, because this dataset provides extra attributes of the data that the model can learn. Here, we choose the gender of the person attribute as another representation learning task. The expanded model is illustrated in Fig. 11 and shows the simplicity of expanding the proposed network to include additional representation and similarity learning tasks.

The experiment results are summarized in Table 7. As we can see from the table, the expanded model works well on all three tasks. Three types of different semantic representations are learned successfully. However, the unbalanced performance is also presented in this model, i.e. the performance on gender attribute learning is around 11% lower than the performances on the other two tasks.



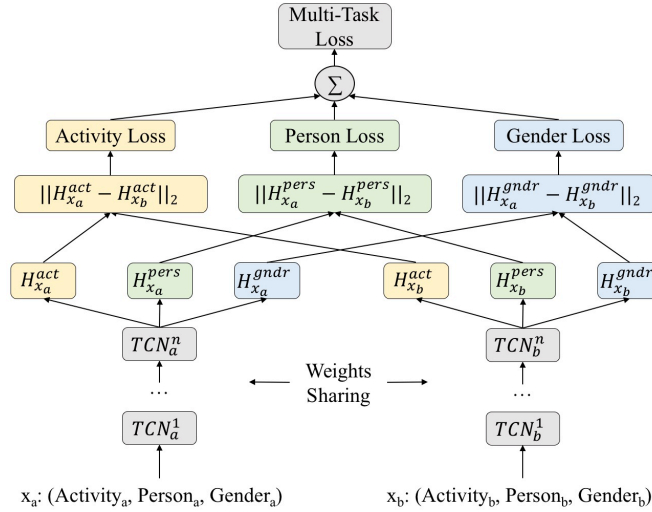


Fig. 11. A tri-output siamese network.

Table 7. Results of proposed multi-task method on PAMAP2 with attribute representation learning in terms of  $F_m$ 

Methods	Activity	Person	Gender
Single-Task Model AR	0.9856	-	-
Single-Task Model PI	-	0.9812	-
Single-Task Model Gender	-	-	<b>0.8678</b>
Proposed Multi-Task Method with Dual-Output	<b>0.9893</b>	<b>0.9881</b>	-
Proposed Multi-Task Method with Tri-Output	0.9798	0.9827	0.8637

## 5 CONCLUSIONS AND FUTURE WORK

In this paper, we propose a weakly supervised multi-output representation learning approach that is built around a siamese architecture consisting of temporal convolutions to capture multiple semantic similarities in the data simultaneously. The clustering results on the learned representations achieved promising performance and even outperformed supervised models in most situations. The visualization analysis demonstrates that the proposed approach succeeds in disentangling the semantic representations, while preserving the similarity metrics in all the representation spaces. Moreover, a series of ablation studies analyzed the effect of the multi-task framework and showed that the use of multi-task training in this architecture most of the time improves performance over single task training, thus illustrating the frameworks ability to efficiently share information between the tasks. Additional experiments showed that the proposed method can also be applied to data with only partial similarity information, can be expanded to learn new, additional task easily, and achieve competitive results in both cases. The comprehensive experiments give useful insights for the proposed multi-task method. Future work will be focused on designing a method that learns to adapt to the unbalancing aspects in the data automatically.

## REFERENCES

- [1] Mohammad Abu Alsheikh, Ahmed Selim, Dusit Niyato, Linda Doyle, Shaowei Lin, and Hwee Pink Tan. 2016. Deep activity recognition models with triaxial accelerometers. In *AAAI Conference on Artificial Intelligence*, Vol. WS-16-01 - WS-16-15. AI Access Foundation, United States, 8–13.

- [2] Ignatov Andrey. 2017. Real-time human activity recognition from accelerometer data using Convolutional Neural Networks. *Applied Soft Computing* 62 (09 2017). <https://doi.org/10.1016/j.asoc.2017.09.027>
- [3] Davide Anguita, Alessandro Ghio, Luca Oneto, Xavier Parra, and J L Reyes-Ortiz. 2013. A Public Domain Dataset for Human Activity Recognition using Smartphones.
- [4] Shaojie Bai, J. Zico Kolter, and Vladlen Koltun. 2018. An Empirical Evaluation of Generic Convolutional and Recurrent Networks for Sequence Modeling. *CoRR* abs/1803.01271 (2018). arXiv:1803.01271 <http://arxiv.org/abs/1803.01271>
- [5] Oresti Banos, Rafael Garcia, Juan A. Holgado-Terriza, Miguel Damas, Hector Pomares, Ignacio Rojas, Alejandro Saez, and Claudia Villalonga. 2014. mHealthDroid: A Novel Framework for Agile Development of Mobile Health Applications. In *Ambient Assisted Living and Daily Activities*, Leandro Pecchia, Liming Luke Chen, Chris Nugent, and José Bravo (Eds.). Springer International Publishing, Cham, 91–98.
- [6] Klas Berggren. 2018. *Human Activity Recognition using Deep Learning and Sensor Fusion*. Master's thesis. Lund University.
- [7] Luca Bertinetto, Jack Valmadre, João F. Henriques, Andrea Vedaldi, and Philip H. S. Torr. 2016. Fully-Convolutional Siamese Networks for Object Tracking. *Computer Vision – ECCV 2016 Workshops* abs/1606.09549.
- [8] Jane Bromley, Isabelle Guyon, Yann LeCun, Eduard Säckinger, and Roopak Shah. 1993. Signature Verification Using a "Siamese" Time Delay Neural Network. In *Proceedings of the 6th International Conference on Neural Information Processing Systems (NIPS'93)*. Morgan Kaufmann Publishers Inc., San Francisco, CA, USA, 737–744. <http://dl.acm.org/citation.cfm?id=2987189.2987282>
- [9] S. Chopra, R. Hadsell, and Y. LeCun. 2005. Learning a similarity metric discriminatively, with application to face verification. In *2005 IEEE Computer Society Conference on Computer Vision and Pattern Recognition (CVPR'05)*, Vol. 1. 539–546 vol. 1. <https://doi.org/10.1109/CVPR.2005.202>
- [10] Seham Abd Elkader, Michael Barlow, and Erandi Lakshika. 2018. Wearable Sensors for Recognizing Individuals Undertaking Daily Activities. In *Proceedings of the 2018 ACM International Symposium on Wearable Computers (ISWC '18)*. ACM, New York, NY, USA, 64–67. <https://doi.org/10.1145/3267242.3267245>
- [11] Davrondzhon Gafurov and Einar Snekkenes. 2009. Gait Recognition Using Wearable Motion Recording Sensors. *EURASIP Journal on Advances in Signal Processing* 2009, 1 (07 Jun 2009), 415817. <https://doi.org/10.1155/2009/415817>
- [12] S. Ha and S. Choi. 2016. Convolutional neural networks for human activity recognition using multiple accelerometer and gyroscope sensors. In *2016 International Joint Conference on Neural Networks (IJCNN)*. 381–388. <https://doi.org/10.1109/IJCNN.2016.7727224>
- [13] S. Ha, J. Yun, and S. Choi. 2015. Multi-modal Convolutional Neural Networks for Activity Recognition. In *2015 IEEE International Conference on Systems, Man, and Cybernetics*. 3017–3022. <https://doi.org/10.1109/SMC.2015.525>
- [14] Nils Y. Hammerla, Shane Halloran, and Thomas Plötz. 2016. Deep, Convolutional, and Recurrent Models for Human Activity Recognition Using Wearables. In *Proceedings of the Twenty-Fifth International Joint Conference on Artificial Intelligence (IJCAI'16)*. AAAI Press, 1533–1540. <http://dl.acm.org/citation.cfm?id=3060832.3060835>
- [15] Z. He and L. Jin. 2009. Activity recognition from acceleration data based on discrete cosine transform and SVM. In *2009 IEEE International Conference on Systems, Man and Cybernetics*. 5041–5044. <https://doi.org/10.1109/ICSMC.2009.5346042>
- [16] Javier Hernandez, Daniel J. McDuff, and Rosalind W. Picard. 2015. BioInsights: Extracting personal data from "Still" wearable motion sensors.. In *BSN*. IEEE, 1–6.
- [17] A. Kale, N. Cuntoor, B. Yegnanarayana, A. N. Rajagopalan, and R. Chellappa. 2003. Gait Analysis for Human Identification. In *Proceedings of the 4th International Conference on Audio- and Video-based Biometric Person Authentication (AVBPA'03)*. Springer-Verlag, Berlin, Heidelberg, 706–714. <http://dl.acm.org/citation.cfm?id=1762222.1762314>
- [18] Herman Kamper, Weiran Wang, and Karen Livescu. 2015. Deep convolutional acoustic word embeddings using word-pair side information. *2016 IEEE International Conference on Acoustics, Speech and Signal Processing (ICASSP) (2015)*, 4950–4954.
- [19] Gregory Koch, Richard Zemel, and Ruslan Salakhutdinov. 2015. Siamese Neural Networks for One-shot Image Recognition.
- [20] Jennifer R. Kwapisz, Gary M. Weiss, and Samuel A. Moore. 2011. Activity Recognition Using Cell Phone Accelerometers. *SIGKDD Explor. Newsl.* 12, 2 (March 2011), 74–82. <https://doi.org/10.1145/1964897.1964918>
- [21] Colin Lea, Michael D. Flynn, René Vidal, Austin Reiter, and Gregory D. Hager. 2016. Temporal Convolutional Networks for Action Segmentation and Detection. *CoRR* abs/1611.05267 (2016). arXiv:1611.05267 <http://arxiv.org/abs/1611.05267>
- [22] Colin Lea, René Vidal, Austin Reiter, and Gregory D. Hager. 2016. Temporal Convolutional Networks: A Unified Approach to Action Segmentation. *CoRR* abs/1608.08242 (2016). arXiv:1608.08242 <http://arxiv.org/abs/1608.08242>
- [23] J. Mantyjarvi, M. Lindholm, E. Vildjiounaite, S. . Makela, and H. A. Ailisto. 2005. Identifying users of portable devices from gait pattern with accelerometers. In *Proceedings. (ICASSP '05). IEEE International Conference on Acoustics, Speech, and Signal Processing, 2005.*, Vol. 2. ii/973–ii/976 Vol. 2. <https://doi.org/10.1109/ICASSP.2005.1415569>
- [24] C. McCool, S. Marcel, A. Hadid, M. Pietikäinen, P. Matejka, J. Cernocký, N. Poh, J. Kittler, A. Larcher, C. Lévy, D. Matrouf, J. Bonastre, P. Tresadern, and T. Cootes. 2012. Bi-Modal Person Recognition on a Mobile Phone: Using Mobile Phone Data. In *2012 IEEE International Conference on Multimedia and Expo Workshops*. 635–640. <https://doi.org/10.1109/ICMEW.2012.116>
- [25] Francisco Javier Ordóñez Morales and Daniel Roggen. 2016. Deep Convolutional and LSTM Recurrent Neural Networks for Multimodal Wearable Activity Recognition. In *Sensors*.

- [26] Jonas Mueller and Aditya Thyagarajan. 2016. Siamese Recurrent Architectures for Learning Sentence Similarity. In *Proceedings of the Thirtieth AAAI Conference on Artificial Intelligence (AAAI'16)*. AAAI Press, 2786–2792. <http://dl.acm.org/citation.cfm?id=3016100.3016291>
- [27] Le T. Nguyen, Ming Zeng, Patrick Tague, and Joy Zhang. 2015. Recognizing New Activities with Limited Training Data. In *Proceedings of the 2015 ACM International Symposium on Wearable Computers (ISWC '15)*. ACM, New York, NY, USA, 67–74. <https://doi.org/10.1145/2802083.2808388>
- [28] Jennifer R. Kwapisz, Gary Weiss, and Samuel A. Moore. 2010. Cell Phone-Based Biometric Identification. *Biometrics: Theory Applications and Systems (BTAS), 2010 Fourth IEEE International Conference on*, 1 – 7. <https://doi.org/10.1109/BTAS.2010.5634532>
- [29] V. Ramu Reddy, T. Chattopadhyay, Kingshuk Chakravarty, and Aniruddha Sinha. 2014. Person Identification from Arbitrary Position and Posture Using Kinect. In *Proceedings of the 12th ACM Conference on Embedded Network Sensor Systems (SenSys '14)*. ACM, New York, NY, USA, 350–351. <https://doi.org/10.1145/2668332.2668359>
- [30] A. Reiss and D. Stricker. 2012. Introducing a New Benchmarked Dataset for Activity Monitoring. In *2012 16th International Symposium on Wearable Computers*. 108–109. <https://doi.org/10.1109/ISWC.2012.13>
- [31] Jorge-L. Reyes-Ortiz, Luca Oneto, Albert Samà, Xavier Parra, and Davide Anguita. 2016. Transition-Aware Human Activity Recognition Using Smartphones. *Neurocomput.* 171, C (Jan. 2016), 754–767. <https://doi.org/10.1016/j.neucom.2015.07.085>
- [32] Shibani Santurkar, Dimitris Tsipras, Andrew Ilyas, and Aleksander Madry. 2018. How Does Batch Normalization Help Optimization? In *Advances in Neural Information Processing Systems 31*, S. Bengio, H. Wallach, H. Larochelle, K. Grauman, N. Cesa-Bianchi, and R. Garnett (Eds.). Curran Associates, Inc., 2483–2493. <http://papers.nips.cc/paper/7515-how-does-batch-normalization-help-optimization.pdf>
- [33] Gabriel Synnaeve and Emmanuel Dupoux. 2016. A Temporal Coherence Loss Function for Learning Unsupervised Acoustic Embeddings. In *SLTU*.
- [34] Toshiyo Tamura, M Sekine, M Ogawa, T Togawa, and Y Fukui. 1998. Classification of Acceleration Waveforms during Walking by Wavelet Transform. *Methods of information in medicine* 36 (01 1998), 356–9. <https://doi.org/10.1055/s-0038-1636855>
- [35] Aäron van den Oord, Sander Dieleman, Heiga Zen, Karen Simonyan, Oriol Vinyals, Alexander Graves, Nal Kalchbrenner, Andrew Senior, and Koray Kavukcuoglu. 2016. WaveNet: A Generative Model for Raw Audio. In *Arxiv*. <https://arxiv.org/abs/1609.03499>
- [36] Laurens van der Maaten and Geoffrey Hinton. 2008. Visualizing Data using t-SNE. *Journal of Machine Learning Research* 9 (2008), 2579–2605. <http://www.jmlr.org/papers/v9/vandermaaten08a.html>
- [37] Jindong Wang, Yiqiang Chen, Shuji Hao, Xiaohui Peng, and Lisha Hu. 2018. Deep learning for sensor-based activity recognition: A survey. *Pattern Recognition Letters* 119 (2018), 3–11.
- [38] Fisher Yu and Vladlen Koltun. 2016. Multi-Scale Context Aggregation by Dilated Convolutions. *CoRR* abs/1511.07122 (2016).
- [39] Neil Zeghidour, Gabriel Synnaeve, Nicolas Usunier, and Emmanuel Dupoux. 2016. Joint Learning of Speaker and Phonetic Similarities with Siamese Networks. In *INTERSPEECH*.
- [40] Ming Zeng, Haoxiang Gao, Tong Yu, Ole J. Mengshoel, Helge Langseth, Ian Lane, and Xiaobing Liu. 2018. Understanding and Improving Recurrent Networks for Human Activity Recognition by Continuous Attention. In *Proceedings of the 2018 ACM International Symposium on Wearable Computers (ISWC '18)*. ACM, New York, NY, USA, 56–63. <https://doi.org/10.1145/3267242.3267286>
- [41] M. Zeng, L. T. Nguyen, B. Yu, O. J. Mengshoel, J. Zhu, P. Wu, and J. Zhang. 2014. Convolutional Neural Networks for human activity recognition using mobile sensors. In *6th International Conference on Mobile Computing, Applications and Services*. 197–205.
- [42] Xiang Zhang, Junbo Zhao, and Yann LeCun. 2015. Character-level Convolutional Networks for Text Classification. In *Proceedings of the 28th International Conference on Neural Information Processing Systems - Volume 1 (NIPS'15)*. MIT Press, Cambridge, MA, USA, 649–657. <http://dl.acm.org/citation.cfm?id=2969239.2969312>